

Chapter 2

Tectonical-Geophysical Setting of the Caucasus

2.1 The Origin of the Caucasus, Geological Evolution and Main Features

Many outstanding geologists such as G. V. Abich, I. M. Gubkin, V. E. Khain, K. N. Paffenholtz studied the Caucasus. The Caucasus comprises four main morphological and tectonic units (Khain and Koronovsky 1997): (1) the Ciscaucasian plain (Scythian platform), including the foredeeps of the Greater Caucasus; (2) the Greater Caucasus itself, stretching in a WNW-ESE direction; (3) the Transcaucasian system of intermontane basins, and (4) the Lesser Caucasus with its an arcuate N-convex shape and the most heterogeneous structure. This geological division of the Caucasus is traditional, although it is sometimes modified (Fig. 2.1).

One of the main characteristics of the Caucasus region is the complexity of its active tectonics, which exhibit both compressive structures such as reverse and strike-slip faults, and extensional features, such as normal faults (Rebai et al. 1993).

Today, the origin and evolution of the Caucasus are mainly explained in terms of plate tectonics (e.g., Khain and Ryabukhin 2002). In a brief review, Kopf et al. (2003) noted that the present-day Caucasus is dominated by thrust faulting due to continental collision. From the Jurassic to the Paleogenic eras, subduction of the Tethian seafloor occurred along the southern margin of the Turkish and Iranian blocks, resulting in calc-alkaline arc volcanism and a wide backarc basin system. The spread of the Red Sea began during the Early Miocene, and the Arabian Plate migrated northward, accompanied by a reduction in width of the Tethys. After its closure (~20 Ma), subduction shifted to the north. As a result of the indentation of the Arabian block, the continuous backarc basin was separated, and the oceanic crust only remained in the Black Sea and the southern Caspian Sea. The continuous northward drift of the Anatolian plate led to initial continental collision expressed by the formation of the Lesser Caucasus, and the subsequent resurrection of the Greater Caucasus during the Middle Pliocene. Currently, continental convergence continues at a rate of up to ~30 mm per year along strike slip faults, where most of the modern tectonic activity is localized. For example, the intersection of deep

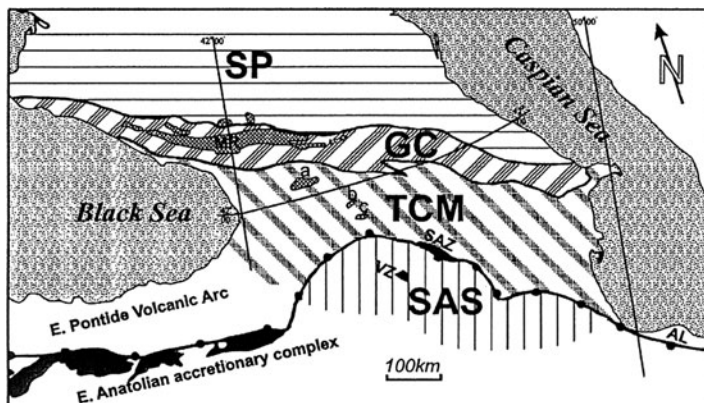


Fig. 2.1 Major crustal units of the Caucasus (After Zakariadze et al. 2007). *SP* Scythian Platform, *GC* Greater Caucasus (*MR* Main Range), *TCM* Transcaucasian Massif ((*a*) Dzirula, (*b*) Khrami, (*c*) Loki salients), *SAS* South Armenian Subplatform, *SAZ* Sevan-Akera ophiolite zone, *VZ* Vedi ophiolite zone, *AL* Albortz Mountains. The line with *black dots* indicates the Eastern Pontide–Lesser Caucasus paleo-oceanic suture zone and corresponds to the southern border of the Eastern Pontide and Caucasus Hercynides

faults was detected at the northern point of sharp tectonic wedge where the destructive Spitak earthquake of 1988 (coordinates: $40^{\circ}49' \text{ N}$, $44^{\circ}15' \text{ E}$) took place (Fig. 2.2).

Gadjiev et al. (1989) identified this feature from this map of the Caucasus (Fig. 2.2) by calculating the lithospheric heterogeneity at different depths. The sum total length of the lineaments within square cells with different sides (corresponding to cubic blocks of different depths) served as a measure of heterogeneity – one that had previously been suggested (Khesin and Metaxas 1974; Khesin 1981).

Note that this map of the deep structure of the Caucasian lithosphere (Fig. 2.2) is consistent with the depiction of horizontal gradients of isostatic and lithospheric gravity anomalies shown in Fig. 2.3.

The presence of a mosaic of microplates in the complex structure of the Caucasus led to additional modifications of plate tectonic theories such as two-stepped plate tectonics (L. I. Lobkowsky) and “shoal tectonics” (I. I. Abramovich), which argues that crust fragments move along inter-crust astenolenses. Shoal tectonics is exemplified by the differences in the Paleogene evolution of the Lesser-Caucasian “andesite belt” between the areas of sluggish crust subduction (Megri-Ordubad Pluton) and the energetic lateral heat/mass transition (Tezhsar Complex in the Pambak ridge).

V. E. Khain (e.g., 1984, 1991–1993, 1995, 2000, 2007) described the geology of the Caucasus extensively. He defined three stages in the evolution of this region during the last 1 Ga: (1) the Baikalian (mainly, the Neoproterozoic) which produced the consolidated basement of the Transcaucasian Massif, (2) the Hercynian (Paleozoic), and the Alpine (Mesozoic-Cenozoic). According to Khain (2000), the most

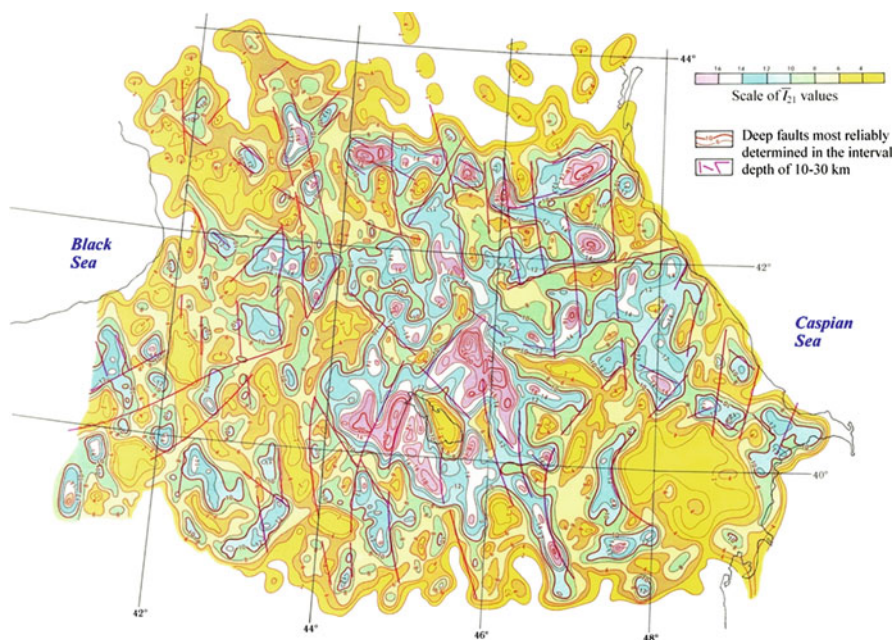


Fig. 2.2 Deep structure of the Caucasian lithosphere (the cut at ≈ 10 km in depth) according to satellite data (After Gadjeiev et al. 1989)

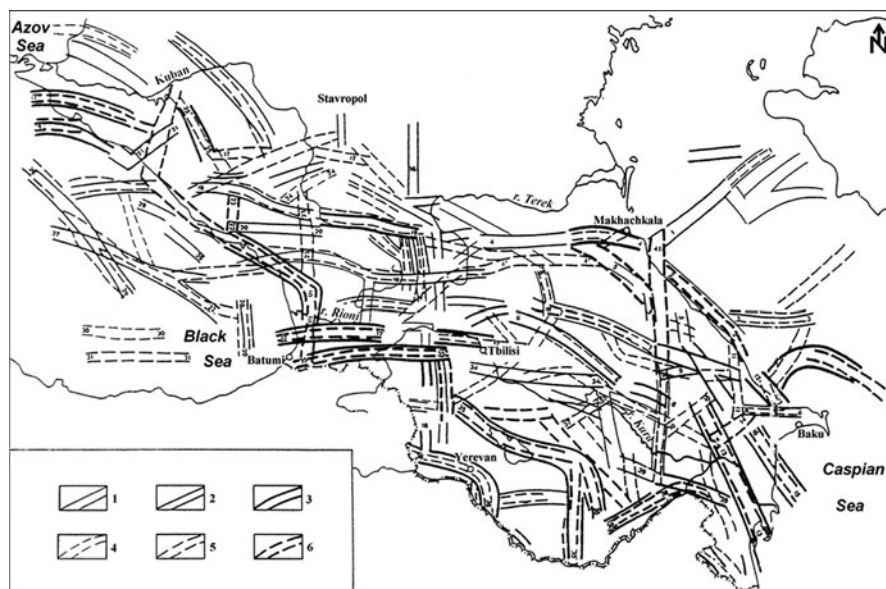


Fig. 2.3 Diagram of horizontal gradients of isostatic and lithospheric gravity anomalies (After Gorshkov and Niauri 1984). Zones of horizontal gradients of isostatic anomalies in mGal/km: (1) 0.5–1; (2) 1–2; (3) 3, zones of horizontal gradients of lithospheric anomalies in mGal/km: (4) 0.5–1; (5) 1–2; (6) 2

ancient Pre-Baikalian structural complex (mainly, gneisses and marbles) is characterized by sub-meridian strikes, often with a declination to the NE. In fact, the deepest earthquakes are linked to the structures of this strike (e.g., Khesin 1976). The less metamorphosed Baikalian complex is rumpled to latitudinal folds in separate areas. The Caledonian complex is practically unknown. The Hercynian complex is characterized by the “Caucasian” (WNW-ESE) strike as are the overlying Mesozoic rocks. Khain and Koronovsky (1997) and Khain (2000, 2007) emphasized the differences in tectonic-magmatic development of the Caucasus in each of the last three stages, as well as the differences between the geological structure of the Ciscaucasus, Greater Caucasus, Transcaucasus, and Lesser Caucasus (Fig. 2.4).

We mainly cite Khain and Koronovsky (1997) in the brief description of these units below.

2.1.1 Giscaucasus

In the southern part of the Ciscaucasian platform, directly adjoining the Greater Caucasus but separated from the latter by a deep fault, is its basement which dates to the Late Proterozoic age and is represented by greenschists and crystalline schists of amphibolite facies. The Upper Proterozoic metamorphic complex is unconformably covered by Ordovician sandstones and Upper Silurian-Lowermost Devonian shales and limestones. This basement is pierced with numerous bodies of K-rich red granites of the Late Paleozoic age.

In the western part of the platform, terrigenous and volcanic Triassic rocks were discovered by drilling. In its eastern part, Triassic strata (the lowermost part of the platform cover) are represented by shallow marine and lagoon deposits of moderate thickness. These deposits are succeeded by sandy-clayey marine Jurassic deposits, with a Kimmeridgian-Turonian evaporate series at the top. Cretaceous deposits are represented everywhere by sandy-clayey-calcareous rocks in the lower part and bedded limestone, marls and chalks in the upper part. The Paleocene-Eocene beds are mainly marly in composition. Above them lies a very conspicuous Maykop series of dark shales (Oligocene-Early Miocene) that was replaced in the Middle Miocene by clays, sands and limestone. A typical coarser molasses (upper molasses) was formed during Upper Miocene, Pliocene and Quaternary eras.

The Kuban Basin in the west and the Terek-Caspian Basin in the east at a depth of 10–12 km or more are mainly filled by the upper molasses. In the Terek foredeep, two parallel lines of anticlines contain large petroleum and gas reserves and extend along the Caspian shore into Dagestan. The Terek foredeep is replaced in north-eastern Azerbaijan by the narrow Kusar-Divitchi foredeep, which is shifted to the south with respect to the former.

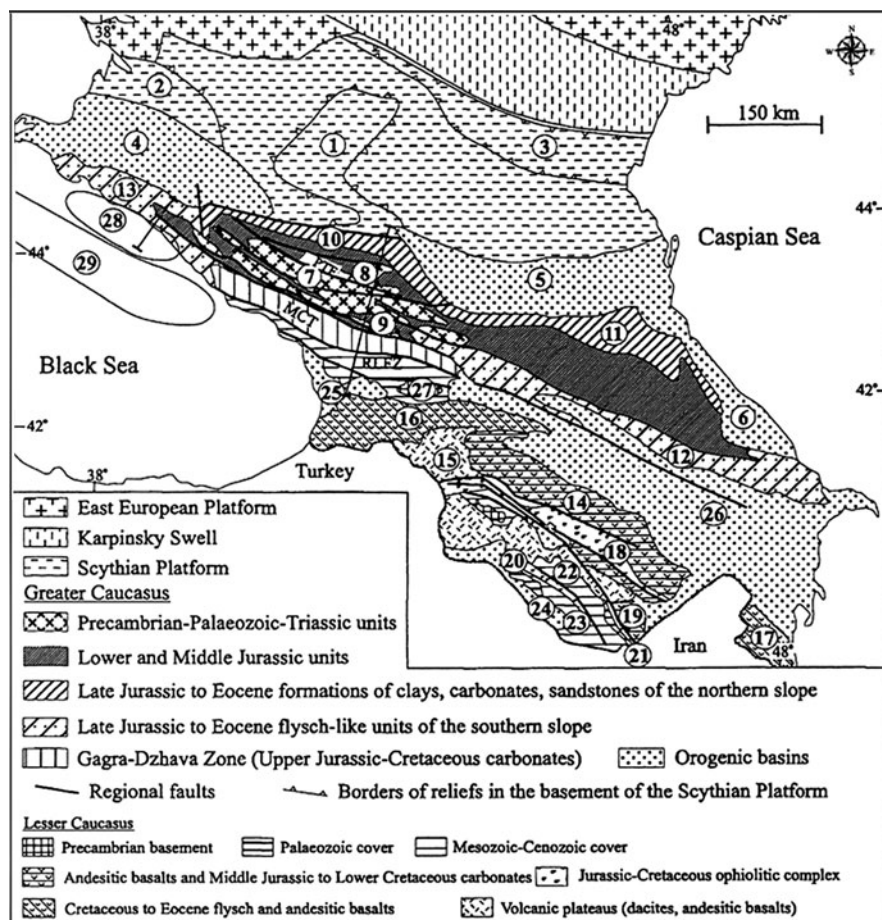


Fig. 2.4 Simplified geological map of the Caucasus (After Milanovsky and Khain 1963; Saintot et al. 2006; with slight modification of the captions). *PTF* Pshkish-Tyrnauz Fault, *MCT* Main Caucasian Thrust, *RLFZ* Racha-Lechkhumi Fault Zone. Circled numbers: 1–6 are zones of the Scythian Platform: (1) Stavropol High; (2) Azov-Berezan High; (3) Manych Basin; (4) Kuban Basin; (5) Terek-Caspian Basin; (6) Kusar-Divitchi Basin; 7–13 are zones of the Greater Caucasus (GS): (7) Peredovoy Zone; (8) Betcha Anticline; (9) Svanetia Anticline; (10) Laba-Malka Monocline; (11) Dagestan Folded Zone; (12) Flysch Zone of southeastern GC; (13) Flysch Zone of north-western GC; 14–24 are zones of the Lesser Caucasus: (14) Somkhet-Karabakh Zone; (15) Artvin-Bolnisi Zone; (16) Adzhara-Trialet; (17) Talysh; (18) Sevan-Akera; (19) Kafan; (20) Vedin; (21) Zangezur; (22) Mishkhan-Zangezur Massif; (23) Ararat-Djulfra Massif; (24) Araks Basin; 25–29 are intramontane zones of the Transcaucasus and Black Sea: (25) Rioni Basin; (26) Kura Basin; (27) Dzirula Massif; (28) Tuapse Basin; (29) Shatsky Ridge

2.1.2 The Greater Caucasus

This mountainous edifice stretches over a distance ~1,300 km and attains a width of 150–200 km in its central part. Its highest summits reach 5,642 m (the comparatively recently (~2000 years) extinct volcano Elbrus) and 5,033 m (another volcano, Kazbek).

The Central Greater Caucasus is divided into three distinct zones: the Peredovoy (Front) Range, Main Range, and the Southern Slope. The Front Range Zone is separated from the Ciscaucasian platform and the Main Range Zone by the deep Northern and Pshkish-Tyrnyauz faults, respectively (Fig. 2.4). In the Front Range Zone, the nappes of northern vergence are composed of ophiolites (probably Early Paleozoic), Devonian island-arc volcanics and Famennian-Lower Visean limestone. A tectonic window of crystalline schists and gneisses of the probable autochthon exists in western part of the zone. Its neo-autochthon is represented by superimposed synclines of Upper Paleozoic molasses that are coal-bearing in the lower part (C_2). Terrigenous Lower-Middle Jurassic with some volcanics lies unconformably on all the older rocks. It is worth noting that the fragments of Early-Hercynian copper-sulphide island-arc system can be seen within the nappes of the Front Range and Main Range.

The Main Range Zone is made up of a complex of crystalline schists and gneisses of amphibolite facies and a K-Na granite series: the metaterrigenous (probably a Lower Paleozoic age) and metavolcanic (Middle Paleozoic) series. The structure of the zone domes and swells formed by crystalline rocks are separated by narrow, steep graben-synclines filled by Lower-Middle Jurassic black slates with some intermediate and felsic volcanics. Marine Permian deposits overlie unconformably the crystalline complex at the southern border of the Main Ridge Zone.

The Main Ridge Zone is thrust to the south onto the Southern Slope Zone. The zone was built up mainly by a very thick sequence of Lower and Middle Jurassic black slates with subordinate volcanics: felsic at the base, diabase-spilite in the Middle and Upper Liassic, and intermediate or felsic in the Aalenian. In Svanetia, Triassic and Paleozoic rocks appear under the Jurassic ones. A thick Upper Jurassic-Cretaceous-Lower Paleogene flysch series conformably overlays the Jurassic formation. This entire complex experienced intense deformation mostly in Late Miocene times and is crumpled in narrow isoclinal folds, divided by overthrusts with a general southern vergence. The zone terminates in the south by a large overthrust where it bounds with the Gagra-Dzhava Zone, which is transitional to the Northern Transcaucasus.

The Gagra-Dzhava Zone is characterized by an ancient crystalline basement and the development of a so-called porphyritic, island-arc volcanic Bajocian series, Bathonian coal measures, Kimmeridgian-Tithonian red beds that are replaced with Upper Jurassic reef limestones in the north, and marly-calcareous Cretaceous and Lower Paleogene series.

In the axial part of the eastern segment of the Greater Caucasus, the Lower-Middle Jurassic slate formation is very tightly folded into two narrow anticlinoria – the Main Range and the Side Range, divided by an even narrower synclinorium. To the north of the Side Range the Upper Jurassic reef formation expressed in the relief by the Rocky Range, is succeeded by Lower-Cretaceous-Cenomanian terrigenous-carbonate, Upper-Cretaceous carbonate and Lower Paleogene marly series. This whole sequence occupies a large strip of Dagestan, where it is folded in a series of box-shaped anticlines divided by narrower synclines.

In Azerbaijan, the Greater Caucasus edifice plunge under the Kusar-Divitchi foredeep. The synclinatorium between the Side Range and Main Range is filled by the Cretaceous wildflysh. The main flysch zone of the southern slope enlarges, and the eastern end of the Gagra-Dzhava (here termed Kakheta-Vandam) zone plunges under a thick Oligocene-Miocene unconformable series overlain by Pontian (uppermost Miocene) and Ahchagyl (Upper Pliocene) beds. This is the Shamakha-Qobustan Zone, separated from the Lower Kura molasses basin in the south by the overthrust. Pliocene deposits comprising the petroleum-rich Productive (or Balakhan) Series at their base occupy most of the surface of the Absheron Peninsula and Caspian shore to the south of it. Older rocks appear here in the cores of diapiric anticlines and mud volcanoes are abundant.

Similar changes took place along the strike of the Greater Caucasus edifice in the western direction, but over a shorter distance and accordingly more abruptly.

In the southern slope of the Greater Caucasus, copper-pyrrhotite stratiform and vein ores within Jurassic slates (e.g., Filizchay or Djikhikh deposits in Azerbaijan) were not initially considered to be a significant source of mineral resources. However, geological-geophysical studies, beginning in the middle of twentieth century revised this opinion (see Sect. 2.2.2).

2.1.3 *The Transcaucasus*

The Dzirula salient of the pre-Mesozoic basement within the Northern Transcaucasian intermontane region represents a zone of transverse Okriba-Dzirula uplift (salient), which divides the main molasses basins into the Rioni Depression in the west and the Kura Depression in the east (see Figs. 2.1 and 2.4). The Upper Precambrian crystalline schists, paragneisses and amphibolites of the salient are the oldest. On them are thrust rocks composed of a Lower or Middle Paleozoic meta-ophiolitic *mélange*. Both complexes are intruded by Late Paleozoic granites and overlain by Late Viséan – Early Serpukhovian acid tuffs. A Mesozoic-Cenozoic cover overlays these Paleozoic rocks with a strong unconformity, beginning with Liassic-Aalenian terrigenous and carbonate deposits, Bajocian island-arc intermediate volcanics (“porphyritic series”), Bathonian limnic coal measures and Kimmeridgian-Tithonian red beds including alkaline basalts. In the west there are also Upper Jurassic evaporites, Cretaceous-Lower Paleogene limestones and marl strata, including Cenomanian volcanics. All these folded strata plunge under the younger deposits of the Rioni and Kura Basins. Oligocene-Miocene deposits fill two narrow troughs on the northern and southern periphery of the Okriba-Dzirula uplift, corresponding to seaways which connected the Rioni and Kura molasses basins up to the Late Miocene.

The Rioni Basin is not as deep (up to 9 km according to geophysical data) and is structurally simpler than the Kura Basin. The main phase of deformation took place in the Late Miocene, and younger deposits lie almost horizontally, except at the southern border of the basin, where the Adzhara-Trialet folded system of the NW framing of the Lesser Caucasus is thrust over the Pliocene deposits.

The Kura Basin extends from the Dzirula Massif to the Caspian shore and continues offshore in the South Caspian deep basin. This basin can be divided into two sub-basins (depressions) – the Middle Kura and Lower Kura, which differ in their width and inner structure. The Middle Kura Depression is bordered on the north by the Gagra-Dzhava marginal zone of the Greater Caucasus and its semi-buried eastern extension and on the south by the Adzharo-Trialet folded system and the northwestern slope of the Lesser Caucasus. The depth of the premolasse basement increases to the east, reaching 15 km according to geophysical data. In the west, the molasses only comprises Oligocene-Miocene marine beds that were folded by the end of the Miocene or the beginning of the Pliocene, whereas in the east they are supplemented by a very thick series of predominantly coarse clastic (partly continental, partly very shallow marine) strata of the uppermost Miocene-Lower Pleistocene, folded by the time of the Middle Pleistocene.

The Lower Kura Depression is bordered on the north by the Shamakha-Qobystan Zone of the southeastern Greater Caucasus. The main part of this depression, between the lower course of the Kura river and the foothills of Greater Caucasus, is filled with a very thick series of Oligocene-Quaternary deposits (including the Lower Pliocene Productive Series), that was deformed in the Middle Pleistocene into several strings of brachyanticline bearing large mud volcanoes. These strings continue in the Caspian offshore, where the mud volcanoes are expressed by islands or submarine rises. The strike of the anticline zones comes progressively closer to meridional offshore. Only the northernmost folds of the Absheron offshore preserve their “Caucasian” WNW-ESE strike and continue with it to the east, forming the Absheron Sill in the sea bottom relief between the Middle Caspian and the South Caspian Basins. The thickness of the sedimentary cover in the South Caspian Basin is very great. The Productive Series contains large petroleum and gas deposits here as well as on shore.

Southwest of the Lower Kura Valley the thickness of the Oligocene-Quaternary deposits diminishes, partly due to the wedging out of the Productive Series. Near the confluence of Kura and Araks a large buried salient of deep rocks was formed by the Talysh-Vandam gravity maximum (Fedynsky 1937), where later the first Soviet super-deep (SD-1) borehole was planned.

2.1.4 The Lesser Caucasus

The Lesser Caucasus comprises parts of the former North Transcaucasian and Iranian microcontinents and remnants of the oceanic basin separating them. The Somkhet-Karabakh zone of the Transcaucasian microcontinent (the Transcaucasian Massif) was uplifted in the post-Eocene and is characterized by the echeloned Shakhdag, Mrovdag and Karabakh ridges that are more than 3 km in height. Metamorphic rocks of the Pre-Mesozoic basement constitute outcroppings in the

Khrami and Loki, and other minor salients and are, in general, similar to the rocks of the Dzirula salient. A thin Lias-Aalenian terrigenous sequence at the base of the Mesozoic section is covered by a thick Bajocian-Bathonian arc volcanic series. The Middle Jurassic volcanism was followed by Bathonian-Neocomian granite intrusions. In the Late Jurassic, reef carbonates accumulated along the NE slope of the volcanic arc and evaporates formed behind them. Then, a new volcanic arc appeared, superimposed on the Middle Jurassic arc. After the cessation of island-arc volcanism in the middle of the Senonian, a cover of Upper Senonian limestone and Lower Paleogene marls accumulated in the Somkhet-Karabakh zone.

The Middle Jurassic volcanics of the Somkhet-Karabakh zone are bordered in the south and south-west by overthrusts of the Sevan-Akera paleo-oceanic zone (Fig. 2.4) which is remarkable for the development of ophiolites. These ophiolites date to the Late Paleozoic and Mesozoic up to Cenomanian. They form tectonic nappes and were obducted on the Transcaucasian and Iranian continental blocks during the Turonian-Coniacian. Then, Senonian general subsidence caused the accumulation of the limestone formations mentioned earlier.

The southernmost zone of the Lesser Caucasus belongs to the former Iranian microcontinent or, according to another opinion, to a separate continental block. Its basement is exposed in the Mishkhan and Western Zangezur massifs and is represented by different metamorphic schists, amphibolites and marbles (Late Proterozoic or earliest Paleozoic?) with intrusive bodies of plagiogranites. A younger Aparan metamorphic series has been identified in the Mishkhan Massif. Both metamorphic complexes are cut by Late Jurassic– Early Cretaceous granitoids, transgressively covered by Upper Cretaceous limestone. To the south and south-west of the belt of metamorphic massifs, a Devonian-Triassic sequence of terrigenous (in the lower part) and carbonate (in the upper part) deposits are widely developed. At its top, coal-bearing beds are present. The Upper Carboniferous is missing, and Permian beds cover the Lower Carboniferous with a crust of weathering at their base. The Mesozoic sequence, lying unconformably on the Paleozoic-Triassic, includes Middle Jurassic marls, Upper Cretaceous limestone, Paleocene flysch and Eocene intermediate volcanics. This sequence of the Yerevan-Ordubad (Ararat-Djulf) Zone is supplemented in the vicinity of Yerevan by a shallow marine sandy-clayey Oligocene.

Eocene magmatic activity was not confined solely to the Yerevan-Ordubad Zone, but rather was widespread throughout the central and southern Lesser Caucasus. Among the plutons, most belong to the granitoid family, e.g., the large Dalidag Pluton in the eastern part of the Sevan-Akera zone, or the even larger and polyphase Late Eocene-Miocene Megri-Ordubad Pluton in the northeastern part of the Yerevan-Ordubad Zone. A pluton of nepheline syenites has been identified in the Pambak Ridge to the west of Lake Sevan.

The formation of the modern structure of the Lesser Caucasus and its general uplift began toward the end of the Eocene. In the Early Miocene the formation of superimposed structures began. The largest of these basins is the Araks (Middle Araks) Basin. These basins contain lacustrine, shallow marine and evaporitic Miocene sediments with embryonic manifestations of halo kinesis.

In the latest Miocene, Pliocene and Pleistocene a vast area of the southwestern part of the Lesser Caucasus became an arena of strong volcanic activity, forming extensive lava plateaus continuing to the west in Eastern Anatolia. Several strato-volcanoes emerged amidst these plateaus; the highest is Mt. Aragats in Armenia (4,095 m).

The Adzharo-Trialet and Talysh Zones (Fig. 2.4) are set apart in northwest and southeast periphery of the Lesser Caucasus, respectively, but have much in common. The Adzharo-Trialet ridge, with summits up to 2,850 m was built up by Albian-Lower Senonian island-arc volcanics, Upper Senonian limestone, Paleocene-Lower Eocene tuffaceous flysh, and Middle-Upper Eocene subalkaline and alkaline intermediate volcanics. The latest Eocene folding was accompanied by small syenite-diorite intrusions. The Talysh Mountain fold Zone, which is elevated up to 2.4 km, does not belong to the Lesser Caucasus proper, because it is separated from it by the Lower Araks Oligocene-Quaternary northeastern strike depression, a branch of the Lower Kura Depression. The oldest rocks exposed in the Talysh are Upper Cretaceous limestone, followed by Paleocene-Lower Eocene tuffaceous flysch, in turn unconformably overlain by Middle-Upper Eocene subalkaline and alkaline andesite-basalt volcanics. The whole sequence is very similar to that of the Adzharo-Trialet Zone. Similarly, the Talysh experienced intense deformation, including the formation of nappes of northern vergence by the end of the Eocene. Thick Oligocene-Miocene molasses accumulated to the northwest and north of the uplifted part of the Talysh. They were folded and thrust to the north on more recent strata of the Lower Kura Depression in the latest Miocene era.

Many renowned specialists have studied the metallogeny of the Caucasus, including Abdullayev (Abdullayev et al. 1962), Magakyan (1961), Smirnov (1978), G. Tvalchrelidze (1976), A. Tvalchrelidze (2002), and their disciples. The Somkhet-Karabakh Zone (Fig. 2.4) with its numerous ore deposits and in particular the well-known Dashkesan-Kedabek (Gedabey) ore region have been the most extensively investigated. The copper-pyrite (sulphide) ores in the Alaverdy and Gedabey deposits, the magnetite ores in the Dashkesan iron deposit have been exploited for decades. The Dashkesan deposit was the sole source of cobalt for the Soviet industry during the Second World War. The pyrite stocks of the Gedabey deposits (in exocontact with the Gedabey intrusive) in the upper horizons converse to copper-pyrite and copper-zinc ores. Most geologists believe that the pyrite ores of the Lesser Caucasus are related to small Later Bajocian sub-volcanic rhyolite-dacite (quartz-plagioporphry) bodies, whereas the copper-pyrite and copper-zinc ores are connected to the postmagmatic activity of the Gedabey intrusive.

Commercial iron, cobalt and alunite ores in Upper Jurassic carbonate-pyroclastic rocks are located in exocontact with the Dashkesan polyphase intrusive. A characteristic feature of the Dashkesan iron deposits is their virtually horizontal bedding of magnetite ores. Mustafayev (2001) suggested that this feature can be attributed to the formation of the Dashkesan intrusive in the synclinorium, unlike the similar intrusives in positive structures of the Lesser Caucasus; in the Dashkesan area, a strain in continental rifting generated sub-horizontal brecciated zones on contacts of rocks with different compositions. Sheet-like and lens-like iron

bodies were formed from hydrothermal solutions within these weakening zones, and skarn-magnetite mineralization was overlapped on the earlier massive ores.

Modern studies of copper mineralization revealed the Karadagh-Kharkhar copper-porphyry field. This field is composed of the rocks of the Atabek-Slavyanka plagiogranite intrusive that is intruded by small dike-like and stock-like bodies of intermediate-basic composition. These small intrusives (quartz-diorite-porphyrates) correlate with sub-meridian fault zones and control the quartz-pyrite-molybdenite and quartz-pyrite-chalcopryrite vein-disseminated ores (Baba-Zadeh et al. 1990).

Gold mineralization in the Azerbaijan part of the Somkhet-Karabakh Zone kindled great interest when information became available about significant gold extraction (about 5–7 t) from the copper-sulphide ores of the Gedabey deposit by the German firm Siemens, which owned copper concessions until to the 1920s. However, no commercial gold-bearing mineralization was actually found. Only modern geological-geophysical efforts designed to study porphyry copper and other mineralization have located any significant sources, e.g., in the Chovdar site.

Gold in the form of admixtures is present in all the copper-porphyry deposits of the Lesser Caucasus. Gold mineralization is distributed broadly by auriferous gravels of the Upper Quaternary alluvial deposits of the rivers flowing from the northeastern slope of the Lesser Caucasus. Gold mineralization was also found in barite-polymetallic veins of the Chovdar deposit (northward Dashkesan) with barite resources of more than 1.5 million tons. The barite-bearing strip on the northeastern slope of the Lesser Caucasus has about 20 deposits and manifestations within fault and fracture zones in anticline arches; the host rocks are Middle-Upper Jurassic volcanics.

The Chovdar goldfield spatially coincides with barite deposits of the same name and series of copper-sulphide, hematite and polymetallic occurrences, as well as gold placers within the northern part of the Dashkesan Mining District. The Chovdar deposit is related to a volcanic-dome structure located at the intersection node of the northwestern and northeastern disjunctive dislocations. Sub-volcanic rhyolite and rhyolite-dacite bodies caused intensive hydrothermal alterations of the Middle and Upper Bajocian volcanics along fault zones with high angle dips. Ore concentrations are found within the porous-fractured secondary quartzite (primarily, quartz-porphyrates) under tuffaceous or porphyritic compact rocks, or in barite/polymetallic veins. Intensive pyritization occurred over polymetallic mineralization (down to a depth of 50–80 m). The polymetallic ores contain sphalerite (mainly), galena (less) and chalcopryrite (infrequently). Recent prospecting work has revealed a new gold-barite-polymetallic mineralization near the villages of Laish and Chovdar within the Kheirachay (Chovdarchay) basins and Goshgarchay Rivers. In the first basin, linear-isometric ore-bodies of irregular shape were contoured within secondary quartzite with a gold content up to 14.4 g/t. Gold content up to 6.2 g/t was detected in barite veins localized in the ruptures of the northwestern strike. In the second basin, the same maximal gold content (6.2 g/t) was detected in vein-lens-like bodies.

The copper-gold mineralization of Kuroko (Lesser Caucasian, according to Tvalchrelidze (1976)) is represented by sheet-like and lens-like bodies, as a

Madneuli deposit in Georgia and in the Kyzyl-Bulakh (“Gold Spring”) deposit in Azerbaijan. In similar deposits, the gold mineralization is concentrated in comparatively narrow and extended zones of hydrothermally altered rocks. Gold mineralization was also found in the polymetallic veins of the Mekhmana deposit near the intrusive of the same name. In general, gold-polymetallic mineralization is attracted to transverse depressions with relative young acid magmatism.

The Sevan-Akera ophiolite Zone represents the main Tethyan suture zone between Eurasia and the South Armenian Subplatform (Fig. 2.1) is characterized by chromite deposits and manifestations within ultrabasite bodies; mercury and gold are attracted to the intersections of these structures. Polymetals, molybdenum and rare metals are attracted to the Dalidag intrusive. In the Yerevan-Ordubad Zone with its well-known large Co-Mo deposits, there is a potential for copper, molybdenum and other ores connected at contacts of the Megri-Ordubad Pluton, and intersections of sub-meridian and sub-latitude fault zones.

2.2 A Brief History of Geophysical Studies in the Caucasus

2.2.1 *Initial Stage*

The first geophysical measurements in the Caucasus were conducted in the nineteenth century using pendulum instruments for absolute gravity acceleration at several locations including a point near Tbilisi (Gongadze 2006). Measurements of magnetic variations have been made in the Tiflis (Tbilisi) Geophysical Observatory since 1844. Applied geothermic studies in boreholes were initiated in the Absheron Peninsula by Batsevich (1881) and further work was done by Stopnevich (1913) and Golubyatnikov (1916).

The first findings to emerge from exploration geophysics were collected in Azerbaijan at the Dashkesan magnetite deposit (Somkhet-Karabakh Zone 1923–1924) by the Geological Committee of the USSR. Ortenberg (1930) carried out measurements of the vertical (Z) and horizontal (H) components of the magnetic field and assessed the iron reserves on the basis of interpretative data; the practically horizontal bedding of the magnetite ores required vector magnetic measurements (Fig. 2.5).

Self-potential (SP) measurements were carried out over the Chiragidzor sulfur deposit (central Azerbaijan) for several years (Fig. 2.6). This figure shows that the mining works in the underground shaft distort the observed SP field strongly at the earth’s surface. This testifies to the tight correlation between mining processes and SP anomalies.

L. V. Sorokin, V. V. Fedynsky and A. I. Zaborousky carried out gravity (with an Eötvös variometer) and Z measurements over the Neogene structures of the Absheron Peninsula (Putu, Binagady) and the southeastern Shirvan in the Lower Kura Depression (Neftechala-Babazanan) from 1926 to 1930. The increased

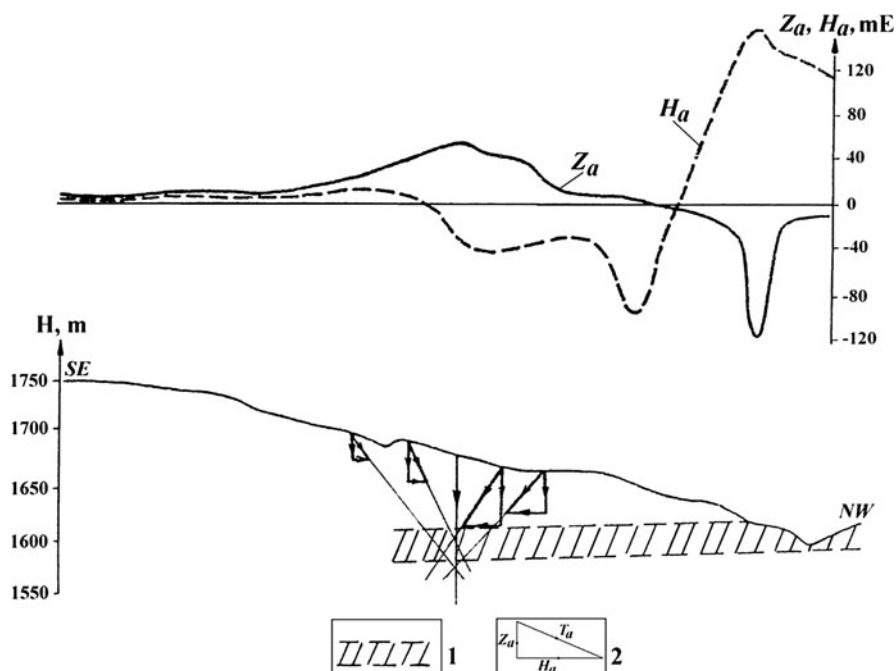


Fig. 2.5 Evaluation of depth of the magnetite bed by the vector technique in the Dashkesan deposit (After Ortenberg 1930). (1) magnetite bed; (2) components of the anomalous magnetic field (T is the total magnetic vector)

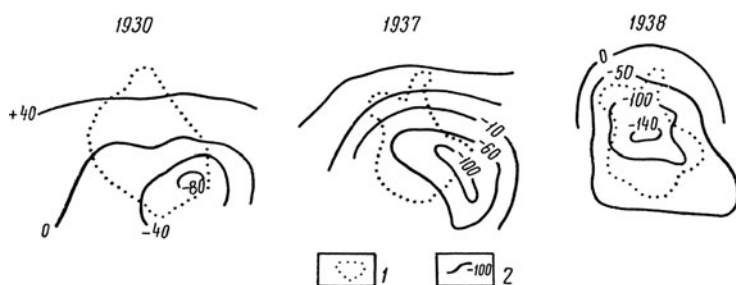


Fig. 2.6 Displacement of SP isolines during exploitation of a new shaft of the Chiragidzor sulfur deposit (Lesser Caucasus) (After Khesin 1969). (1) shaft contour; (2) isolines of SP field (in millivolts)

magnetization of the Productive series, and the gravitational effect of fold arches enabled them to delineate anticline structures and trace disjunctive dislocations. The presence of a Hilly fold in the Lower Kura Depression, contoured by the magnetic prospecting, was then verified by drilling. Roughly at this time

(1929–1934), these pioneers conducted general pendulum gravity (Fig. 2.7) and magnetic T surveys.

The findings of these general surveys revealed the main regional peculiarities of the deep structure of the Caucasus (Arkhangelsky and Fedynsky 1932; Arkhangelsky 1933; Abakelia 1937; Fedynsky 1937; Nodia 1939).

Before as well as during the Second World War several other geophysical studies were conducted. Petrovsky and Skaryatin (1929) successfully applied an ondometric (radiowave) method to the translucent Chiragidzor pyrite stocks in Somkhet-Karabakh Zone (Azerbaijan). Slightly earlier, in the 1930s, a self-potential (SP) survey was also successful in studying these stocks (M. L. Ozerskaya, S. N. Kondrashev, A. G. Surikov).

A new (Toganaly) pyrite deposit was found in the area of SP anomaly in 1938 (Khesin 1962a). In the early 1930s, geophysicists from the French firm Schlumberger introduced the resistivity method of electric prospecting in the Absheron Peninsula. A Buzovny structure was detected here by a reflection survey of seismic prospecting that started in 1935–1936 in southeastern Shirvan (Pirsagat-Khydyrli); a large oil deposit was later revealed in the Busovny anticline (Kerimov 1996). Balavadze (1939) studied Akhaltsikhe coal deposits in Georgia using gravity prospecting. He identified cobalt-bearing veins in the Dashkesan deposit using electric resistivity profiling (Balavadze 1944). A correlation refraction survey method was used in the Absheron Peninsula as early as 1944 (G. A. Gamburtsev and Yu. V. Riznichenko).

2.2.2 *Formative Stage*

After the Second World War and practically until the final years of Gorbachev's "Perestroika" in the USSR, huge geophysical works were carried out in the Caucasus by the central and local prospecting services of the Oil-and-Gas, Geology and other Soviet Ministries, as well as by numerous scientific and educational organizations. During this time mid-scale (mainly, 1:200,000) gravity surveys and aeromagnetic/magnetic surveys were conducted elsewhere, depressions were studied by seismic and electric prospecting (primarily for petroleum exploration), and deep seismic sounding was used to study the Earth's crust. Hundreds of prospective oil-and-gas bearing structures were prepared for deep drilling by large-scale geophysical methods (1:50,000–1:25,000) as well as detailed geophysical studies (e.g., Kerimov 1996). Deep structures were primarily explored through seismic prospecting (Fig. 2.8).

This profile across the Taman mud volcano province shows diapirism attenuation with depth: in the near-arch part of the diapiric fold, dip angles of the reflectors decrease with increases in depth from 50–60° down to 10–5°.

At the same time that these indirect (structural) geophysical explorations of oil-and-gas were being pursued, geophysical methods for direct petroleum prospecting were initiated. The first successful attempts took place in Azerbaijan

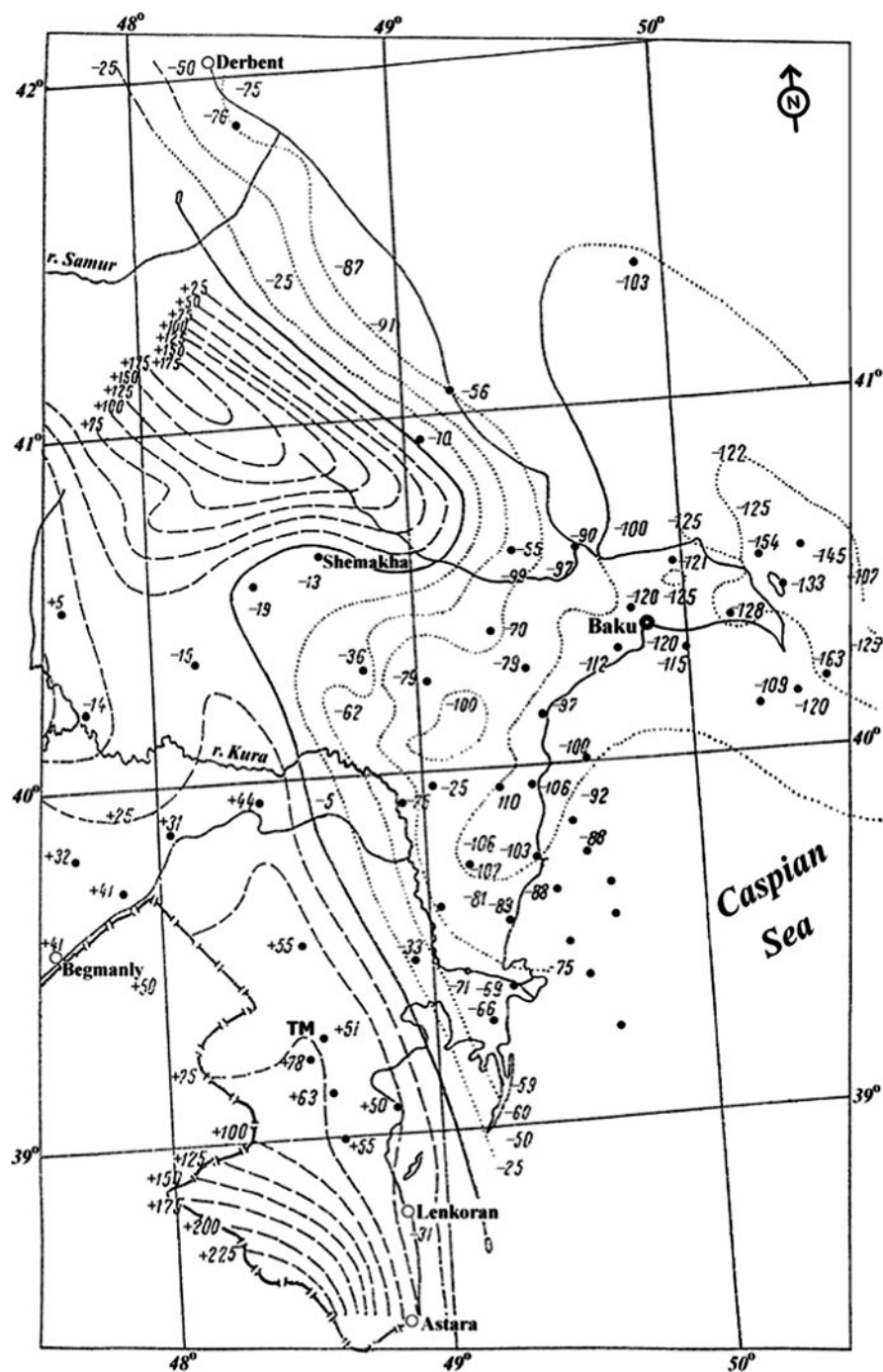


Fig. 2.7 Gravity anomalies (in mGals) in free-air reduction detected by pendulum survey in the Eastern Caucasus (After Fedynsky 1937). Talysh-Vandam gravity maximum is designated as TM

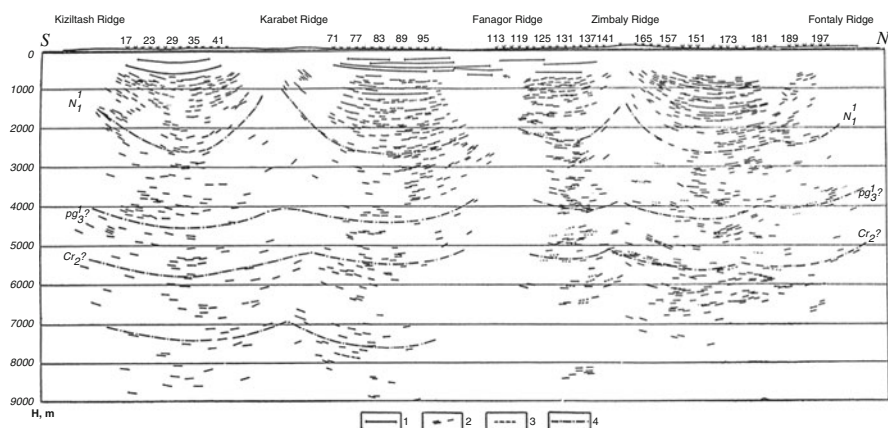


Fig. 2.8 Seismic profile across the Taman Peninsula (Matusevich and Priyma 1967). (1) reflection horizon; (2) reflection pieces; (3) reflection pieces plotted by uncertain reflections; (4) conventional horizon

(I. G. Medousky and others), where zones of seismic wave attenuation were shown to coincide with the contours of oil and gas deposits. The potential of geophysical direct prospecting was clearly demonstrated in the Anastasievskaya fold in the Western Kuban Basin, where gas and oil horizons occur at the depth about of 1–1.5 km (Zemtsov 1967).

In this anticline, reflections from gas-water contact were seen; the local minima of seismic amplitude curves were observed over the productive part of the geological section. These minima correlated with radioactive indications of hydrocarbon presence. Moreover, such indications as the local gravity minimum over the deposit was also recorded. The calculation of the module of the gravity vertical gradient by the Berezkin method (e.g., Berezkin 1988) showed the location of the anomalous source within the main productive interval.

The development of direct petroleum geophysical exploration in the Caucasus was aided considerably by magnetic prospecting using a method developed by Bagin and Malumyan (1976). These researchers identified a magnetite-siderite mineral association within petroleum-bearing and mud volcano deposits of the Productive Series of the Absheron Peninsula, unlike in non-productive deposits. This magnetic association was formed from a reduction of thin-dispersed iron oxides and hydroxides (Pilchin and Eppelbaum 2006) under the influence of hydrocarbons; thus, the application of a magnetic method for direct petroleum prospecting was feasible.

By contrast, the development of mining geophysics in the Caucasus started from direct ore prospecting and later was accompanied by the study of deep structural, magmatic and lithological factors of ore control. Diverse geophysical methods were applied to assess different mineral resources. For example, the SP survey was

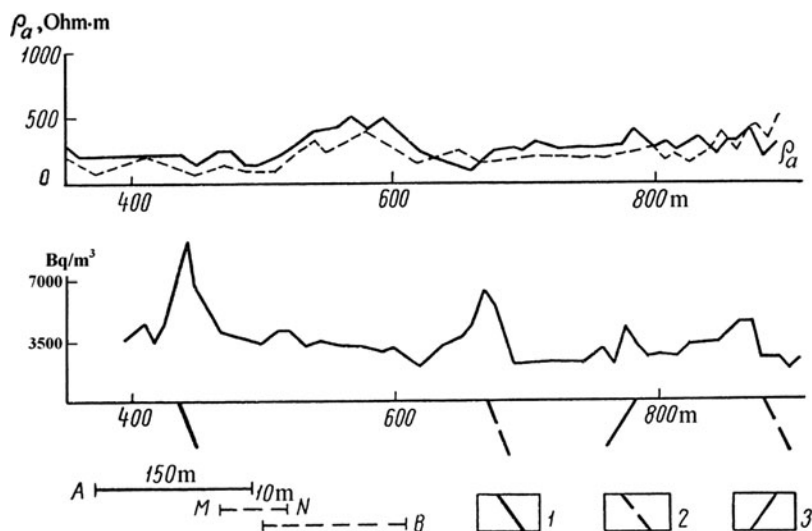


Fig. 2.9 Delineation of cobalt-bearing fragmentation zones by combining data on resistivity profiling and an emanation survey in the Dashkesan ore district (Lesser Caucasus) (After Khesin 1962b, 1969). (1) known cobalt-bearing fragmentation zone; (2) zones of cobalt-bearing fragmentation revealed by geophysical data; (3) contact of tuffaceous suites

continued, and SP anomalies were revealed over copper-sulphide and pyrite stocks of the Gedabey deposits. As of 1959, most of the geophysical studies by the Azerbaijan Geophysical Expedition (AGE) were concentrated in the northwestern part of the Lesser Caucasus in the Dashkesan-Gedabey ore region. In the Dashkesan area, new cobalt-bearing fractured zones were detected by combined electric profiling based on “ore” (direct, “conductive”) intersections of apparent resistivity (ρ_a) graphs and the results of radioactive (radon) surveys (Fig. 2.9).

Combined electric profiling also helped resolve other prospecting problems, including the detection of caoline clays with a resistivity of $60 \Omega \text{ m}$ within the Bajocian effusives with a resistivity about of $1,000 \Omega \text{ m}$ (Fig. 2.10). Figure 2.10 also shows the dip of the kaolinized zones as a function of the displacement of “conductive” intersections for different separations of the current electrodes, i.e., for different probe depths.

During the study of bentonite clays, high-quality bentonites with a resistivity of $1\text{--}2 \Omega \text{ m}$ were separated from low-quality bentonites ($\sim 5 \Omega \text{ m}$).

AGE geophysical surveys were usually integrated with geochemical (metallometric) studies that provided direct indications of different ores. One example is the detection of chromite ores in the Sevan-Akera Zone of the Lesser Caucasus (Fig. 2.11).

The Kuban and Armenian Geophysical Expeditions successfully carried out direct geophysical prospecting of ore deposits as well. For example, electric prospecting of copper-sulphide deposits within the volcanogenic strip of the Northern Caucasus was

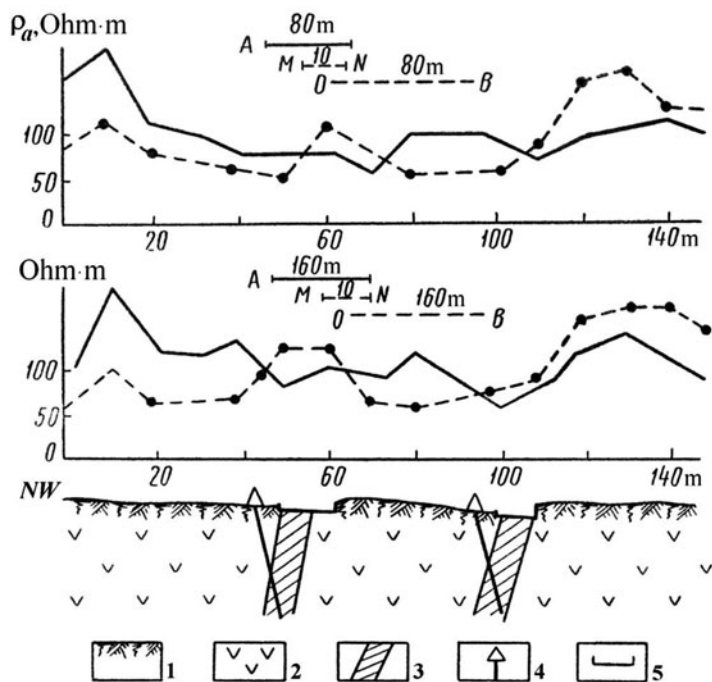


Fig. 2.10 1:5,000 combined profiling implemented for the detection of caolinite clays, in the Chardakhly deposit (Gedabey ore area, Lesser Caucasus) (After Khesin 1969). (1) loose deposits; (2) secondary quartzite; (3) caolinite and refractory clays; (4) borehole; (5) trench

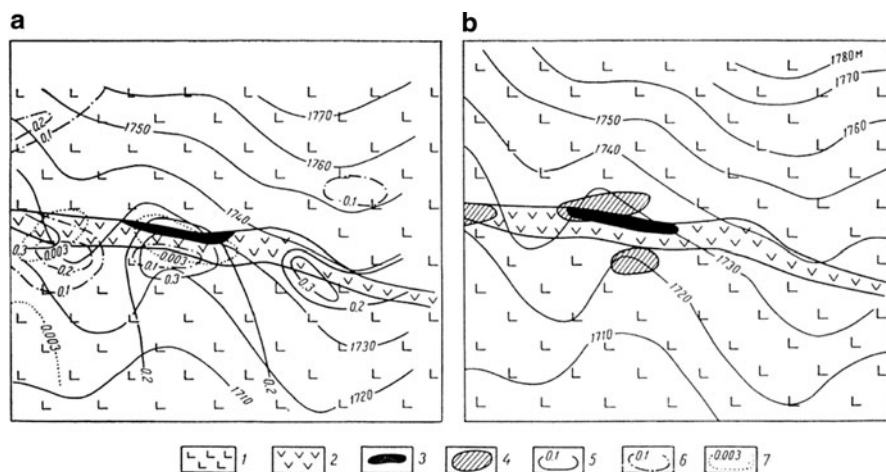


Fig. 2.11 Delineation of chromite-bearing dunites with metallometry (a) and gravity prospecting (b) data (Khesin and Muradkhanov 1962). (1) serpentinized peridotites; (2) serpentinized dunites; (3) chromite ore; (4) gravitational maximums, isoconcentrations (in%); (5) chrome; (6) nickel; (7) zinc

complicated by the presence of mineralized fault zones and graphitized schists of low resistivity. Nevertheless, the resistivity of massive ores ($\rho = 0.02\text{--}0.03 \text{ } \Omega \text{ m}$) is less in the often cited 1–2 ranges above false targets, and these ores were clearly detected at a depth of 70 m by the inductive non-grounding loop method (Fig. 2.12).

Furthermore, the integration of geophysical methods became the main tool for successful prospecting in the complex environments of mountainous ore regions with rugged topography, intense tectonics, a multitude of rock classes and other factors that make the interpretation of geophysical anomalies difficult. The history of discovery of the very large polymetallic-sulphide deposit in the Azerbaijan part of the southern slope of the Greater Caucasus, near the border of Georgia, followed by a new polymetallic province is one of the most impressive of these stories. The 1958 geological survey within the disrupted arch of a near-latitude anticline revealed two small ore outcrops in the Toarcian-Aalenian schists of the Tfan anticlinorium. These outcrops contained a series of ore minerals including pyrite, pyrrhotite, sphalerite, galena, chalcopyrite, and precious metals. An integrated detailed geophysical survey of the AGE in 1960 reported on the magnetic, SP and induced polarization (IP) measurements of apparent polarizability (η_a) (Mustafabeily et al. 1964). This survey showed that these outcrops represented a very large ore-body both in strike and dip. The SP negative anomaly (several hundreds of milliVolts) traced this Filizchay (“Ore river”) ore-body to 1,200 m along the strike (Fig. 2.13).

The SP anomaly could have been caused in this area by a conductive schist, but the nature of the ore in the anomaly was shown to have magnetic anomalies of about 200 nT over the eastern part of the ore-body enriched by magnetic pyrrhotite. On the other hand, the magnetic anomaly in this area might have resulted from a magnetic diabasic (non-conductive) body, but the SP anomaly and the anomaly of η_a up to 30–40% reflected a conductive ore source. The quantitative interpretation of the magnetic anomaly indicated that the depth of the upper edge of the magnetic source was 40–45 m. Subsequent drilling confirmed this calculation to 10% accuracy (Khesin and Muradkhanov 1967).

On the basis of these results, integrated geophysical surveys of the AGE were made on a scale of 1:10,000 for the entire Filizchay ore field and on a large scale for the adjacent territory. These surveys revealed a series of prospective areas and sites, several of which were recognized later as polymetallic deposits. The location of these areas and sites was comparable to some of the features of the regional distribution of geophysical fields (Fig. 2.14).

In the central part of this ΔT map (Fig. 2.14) the near-latitude maximum (Guton maximum) can be seen. This maximum was interpreted as a hidden intrusive body that might affect the mineralization distribution. The largest deposits in the western margin of the anomaly correlated with the transverse dislocation reflected in the strike of the ΔT field. Here, a high dip was also detected in the southeastern flank of the gravity maximum. To evaluate the depth perspectives, area surveys were supplemented by reference regional profiles with IP soundings (Khesin 1969, 1976). This

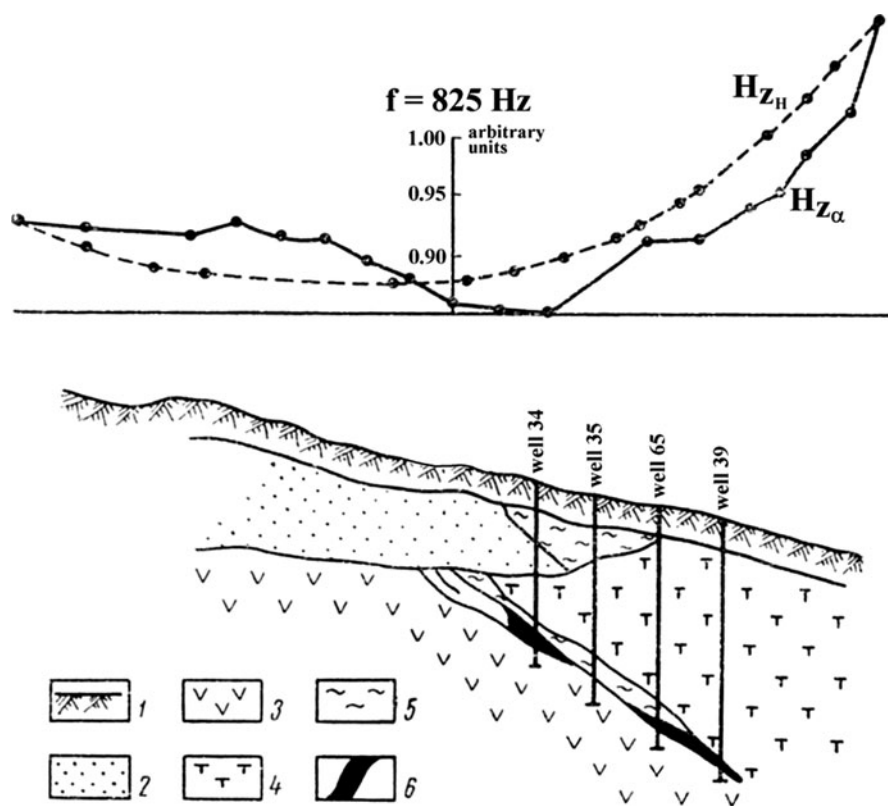


Fig. 2.12 Detection of copper-sulphide ores in the Northern Caucasus by the non-grounding loop method (After Vinogradov 1964). (1) modern deposits; (2) Jurassic deposits; (3) quartz-albitophyres; (4) tuffs of intermediate composition; (5) siliceous schists; (6) massive copper-sulphide ore

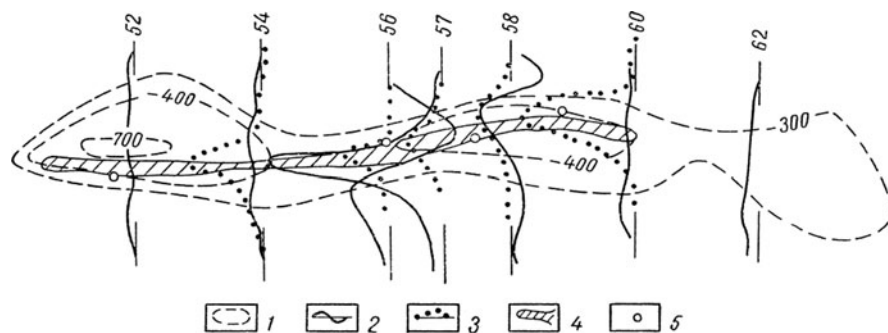


Fig. 2.13 Detection of the Filizchay ore deposit by the integration of geophysical methods (After Khesin and Muradkhanov 1967). (1) isopotentials of the negative SP field (in millivolts); (2) ΔZ graphs; (3) η_a graphs; (4) projection of the upper edge of the ore-body on the plan; (5) boreholes, intersected polymetallic-sulphide ore

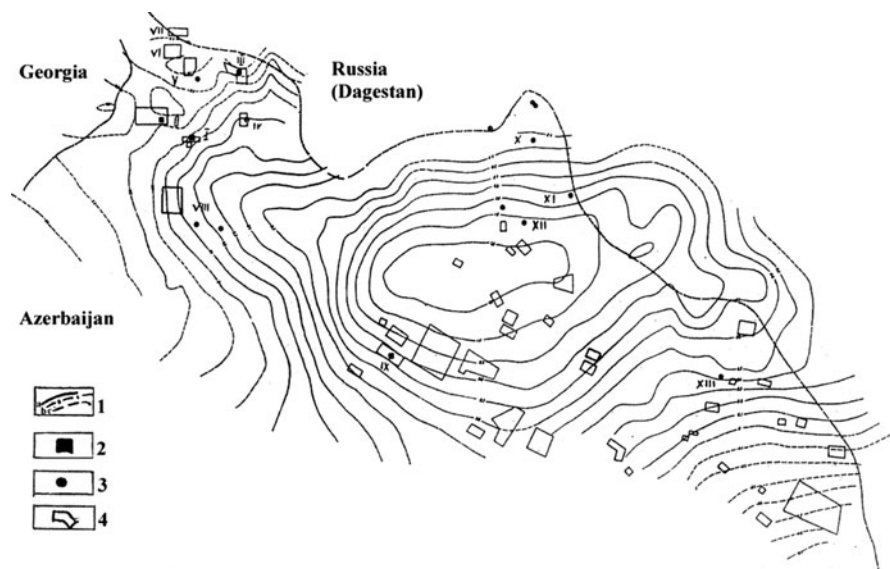


Fig. 2.14 Average results of helicopter magnetic survey and distribution of ore and prospective sites of the Belokan-Zakatala ore region (Modified from Khesin 1976). (1) isodynamas (in nano-Tesla) of the modulus of the full magnetic vector (ΔT): (a) positive, (b) zero, (c) negative; (2) ore deposits; (3) ore manifestations; (4) anomalous sites revealed by large-scale ground and detailed geophysical surveys: (I) site of the Filizchay deposit, (II) site of the Katsdag deposit, (III) site of the Djikhikh deposit, (IV) site of the Katekh deposit

geophysical experience was implemented in adjacent territories and led to the discovery of a large copper-polymetallic deposit (Kyzyl-Dere) in Dagestan.

A similar combination of indirect and direct geophysical prospecting was undertaken in the Lesser Caucasus. In the Shamkhor (Shamkhir)-Gedabey-Dashkesan region of the Somkhet-Karabakh Zone (Fig. 2.4) many geologists have associated its ore potential with different phases of the Dashkesan and some other intrusives. Aeromagnetic data analysis made it possible to detect the hidden intrusive masses (Fig. 2.15).

Integration of geophysical methods including various modifications of seismic prospecting yielded abundant information about the hidden parts of intrusive bodies and other deep peculiarities (Fig. 2.16).

Figure 2.16 shows that seismic prospecting by the reflection and refraction methods clearly outlines the intrusive at a depth, whereas the local fault was detected by the diffraction method. Gravity and magnetic maxima additionally confirmed the presence of dense and magnetic basic intrusive rocks at a depth. Integrated interpretation of seismic and other geophysical data using the information approach (Khesin 1976) also identified a hidden intrusive body in the southern immersion of the Gedabey intrusive (reference profile III-III in Fig. 2.15).

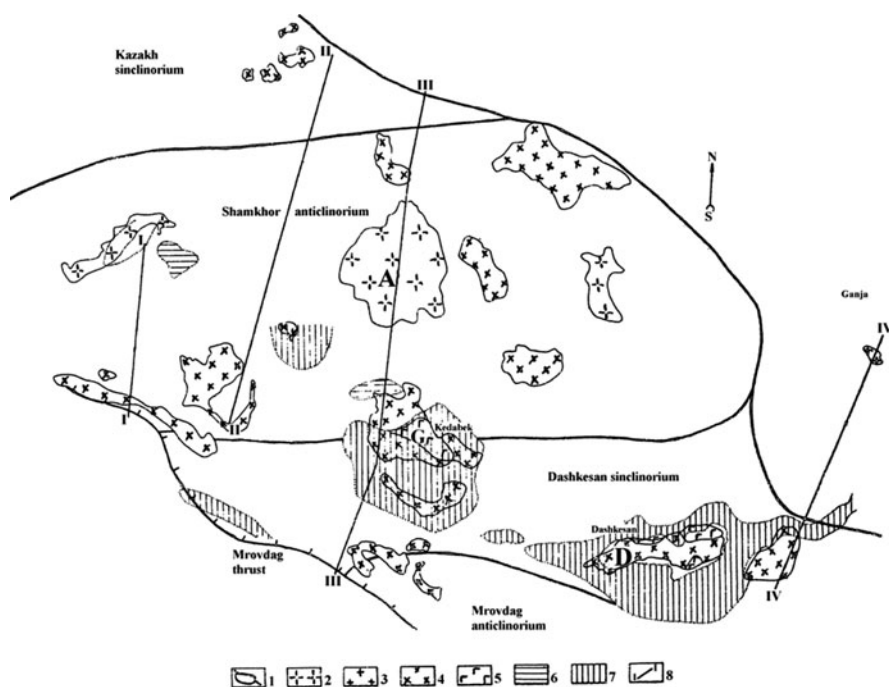


Fig. 2.15 Distribution of intrusive bodies in the northeastern Lesser Caucasus indicated by magnetic data (After Khesin 1976, with supplements). (1) borders of large geostructures; (2) plagiogranites; (3) granites; (4) granodiorites and diorites; (5) gabbroid rocks; (6) granodiorites and diorites; (7) gabbroid rocks detected down to a depth of 0.5 km by airmagnetic data interpretation; (8) location of interpreting profiles. Main intrusive bodies: A Atabek-Slavyanka, D Dashkesan, G Gedabey

2.2.3 Contemporary Period

In the last years of the USSR's existence and the first years after the formation of independent states which replaced the former republics of the USSR, financial and organizational problems curtailed geological-geophysical prospecting considerably. At the same time, growing geophysical data and methodological-technological innovations facilitated new trends. First, the analysis and generalization of the results of geophysical studies led to the publication of major works (e.g., Gugunava 1988; Ismail-Zadeh and Khesin 1989a,b; Kerimov et al. 1989). Second, underground geophysical investigations and the integration of traditional geophysical methods with direct techniques of mineralization detection (e.g., Ryss 1983) were extended. Third, the new kinds of mineral resources within known prospective areas began to be studied (e.g., gold prospecting in relation to porphyry copper studies in the Somkhet-Karabakh Zone), as well as cooperation with firms and organizations from the USA, Europe, Japan and Israel, especially in petroleum exploration.

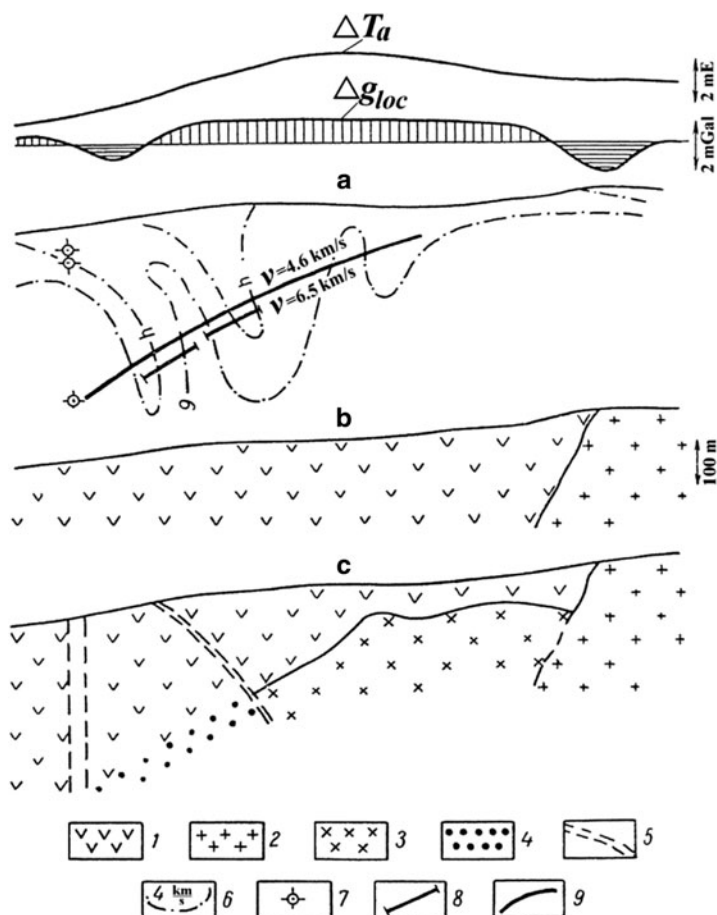


Fig. 2.16 Integration of seismic prospecting with other geophysical methods for the study of a hidden intrusive body to the NW of the Gedabey intrusive, near reference profile II-II in Fig. 2.15 (Khesin 1969, seismic data of A. Sh. Mamed-Zadeh, Yu. G. Shopin and S. A. Miri-Zadeh): (a) aeromagnetic and gravity anomalies over velocity section, (b) geological section, (c) result of interpretation of geophysical data. (1) porphyrites and tuffs of the Lower Bajoicain; (2) intermediate intrusive rocks; (3) basic intrusive rocks; (4) zone of intense contact metamorphism; (5) disjunctive dislocation; (6) isolines of refraction wave velocities (km/s); (7) diffraction point; (8) reflection piece; (9) refractor

Underground geophysical studies revealed new ore-bodies in such old copper-sulphide deposits as Alaverdy in northern Armenia (Somkhet-Karabakh Zone). These copper-sulphide and pyrite ores have low resistivity (on average, 30 Ω m) and high polarizability (on average, 22%), whereas the host tuffites, porphyrites and volcanic breccias have high resistivity (on average, 1,300 Ω m) and low polarizability (Ovsepyan et al. 1986). The results of measurements of the IP, SP

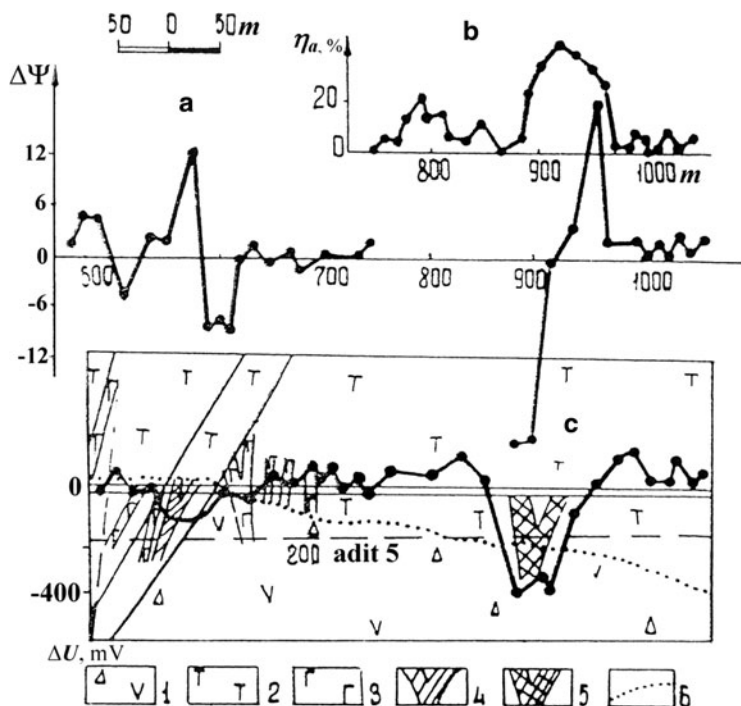


Fig. 2.17 Results of underground electric prospecting in the Alaverdy copper deposit: (a) stray currents, (b) IP, and (c) SP (Ovsepyan et al. 1986). (1) porphyritic breccias; (2) tuffites; (3) andesite-dacite porphyrites, veins; (4) known ore-body; (5) ore-body, revealed by electric prospecting; (6) tectonic dislocation

and stray currents (the latter method provides an ore/host rock conductivity ratio – $\Delta\Psi$) in adit 6 of the deposit are shown in Fig. 2.17.

Figure 2.17 shows that a known ore-body causes the geophysical anomalies in the 580–600 m interval. An intensive SP negative anomaly, $\Delta\Psi$ and η_a anomalies detected a hidden ore-body in the 900–980 m interval under adit 6. This conclusion was confirmed by mining. In this deposit, the polarization curve correlation method (Ryss 1983) enabled the authors to define the spatial distribution and content of copper mineralization with greater precision.

The Karadagh-Kharkhar copper-porphyry field is the most highly studied area of the Azerbaijan part of the Somkhet-Karabakh Zone (Kerimov 1996). Ore-bearing sites are located within hydrothermally altered rocks that were accurately detected by data showing a decrease in magnetic field and resistivity from an integrated geophysical survey on a 1:10,000 scale. The deposit area (400–900 m × 2,200 m) is outlined by a polarizability isoline of 7.5%. Within the contour, local η_a maxima (up to 10–18%) are related to the increase in the concentration of disseminated pyrite and certain other sulphides. These maxima coincide with the SP minima (down – 60 mV). Method of partial extraction of metals (Ryss 1983) applied to the

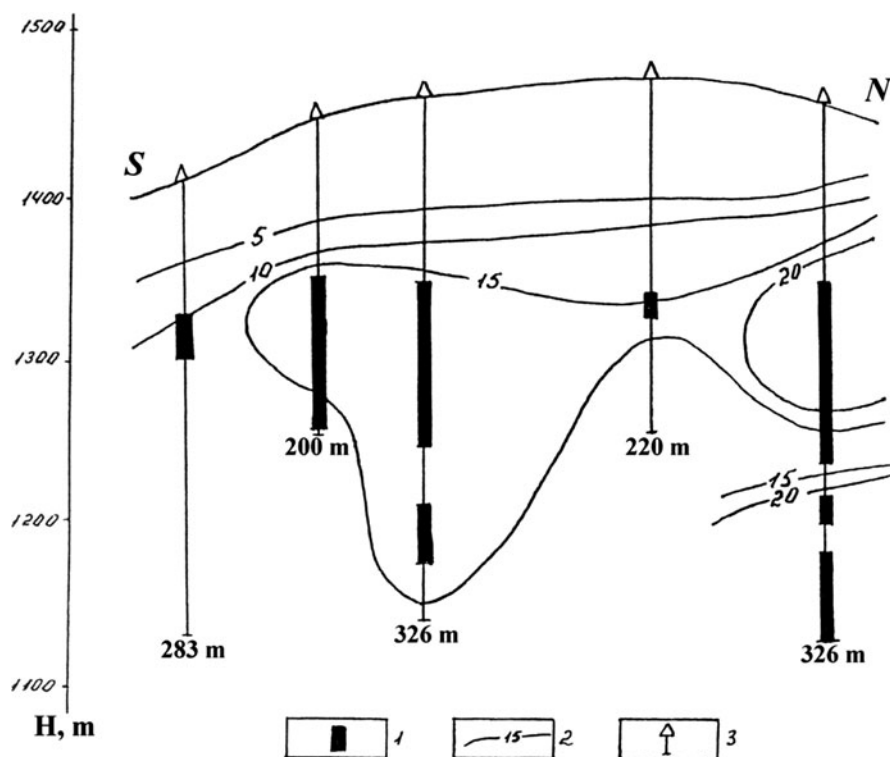


Fig. 2.18 Results of borehole η_a measurements in the Karadagh copper-porphyry deposit (After Bagirov et al. 1996). (1) intervals of commercial concentrations of copper in the drill core; (2) η_a isolines (in%); (3) borehole

sites of the local anomalies showed 30 μg of the copper, 5 μg of the lead and 500 μg of the iron on a background of 5, 2 and 200 μg , respectively. Nuclear geophysical methods were used here for drill core and well studies. They showed copper concentrations of 0.2–0.8%; concentrations of 1.1–1.4% were detected in several borehole intervals at thicknesses of up to 1.5 m. IP anomalies in the wells correlated closely with the ore cuttings (Fig. 2.18).

2.3 The Caucasus in the Light of Regional Geophysical Analysis

The key features of the deep structure of the Eastern Caucasus were first delineated by a pendulum survey that revealed the Talysh-Vandam gravity maximum (see Fig. 2.7). This maximum was shaped like a salient that extended from the

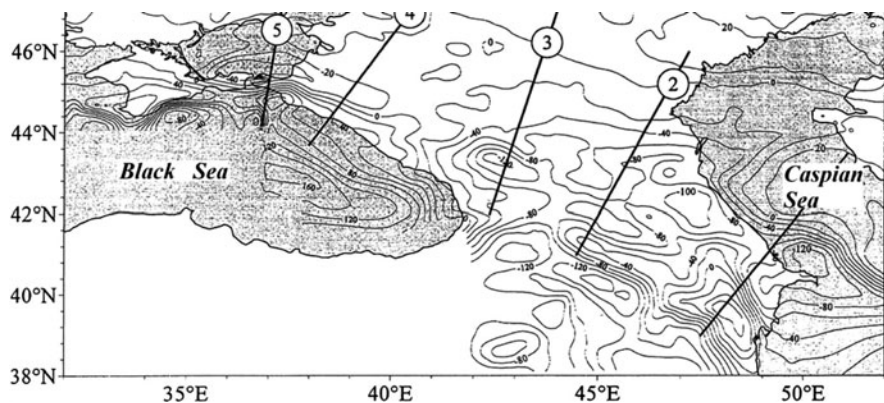


Fig. 2.19 Bouguer gravity anomalies of the Caucasus with isoline interval of 20 mGal (Data from the Geological Survey of Russia)

Near-Talysh Mugan steppe northward across the towns of Kyurdamir, Agsu and Geychay up to Lagich and Vandam. Latter, numerous gravimetric surveys provided a more complete picture of the gravity field (e.g., Fig. 2.19).

Satellite gravity data were obtained from the World Gravity DB as retracked from Geosat and ERS-1 altimetry (Sandwell and Smith 2009). Crucially, these observations were made with regular global 1-min grids (Sandwell and Smith 2009) and the gravity data computation error was estimated at 2–3 mGals. The compiled gravity map (Fig. 2.20) shows the intricate gravity pattern of this area (the isoline interval is 10 mGal; “zero” isoline is dashed and white bolded). This figure demonstrates that in specific cases it is useful to display the gravity field map without any reduction. The selected positive and negative gravity anomalies (Fig. 2.20) clearly reflect the main structural-geotectonical units of the region. Disparities between the free air, the Bouguer gravity map (Fig. 2.19) and the retracked gravity map (Fig. 2.20) can be used to estimate topographic corrections and solve various regional gravimetric problems.

The zones of gravity minima in Fig. 2.19 are related to mountainous edifices of the Greater and Lesser Caucasus, where the depth of the Moho discontinuity is increased. This is clear from the constructed map of Moho discontinuity (Fig. 2.21).

Models of deep structure of the Caucasus were coordinated with the results of deep seismic sounding (DSS); for example, the depths of the Moho discontinuity in the Greater Caucasus along the Grozny-Shamkhor (Shamkir) segment of Volgograd-Nakhichevan (Nakhchivan) DSS profile exceeds 50 km (e.g., Krasnopevtseva 1984).

The Talysh-Vandam gravity maximum was studied by different geophysical methods at different scales. Its characteristics elicited heated debate. Fedynsky (1937), Tzimelzon (1959), Gadjiev (1965) argued that this maximum resulted from the elevation of the crystalline basement and the development of magmatic rocks within the basement and sedimentary cover.

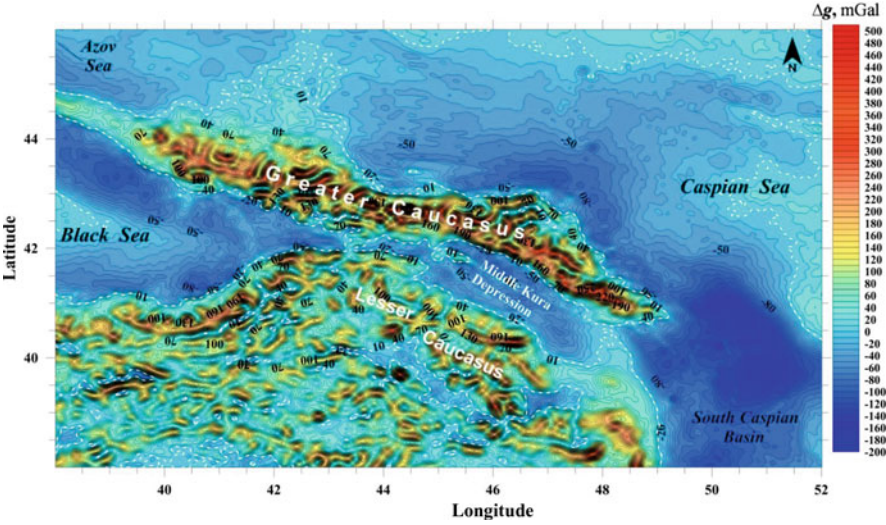


Fig. 2.20 Map of significant gravity anomalies of the Caucasus and adjacent areas (isolines are given in mGals)

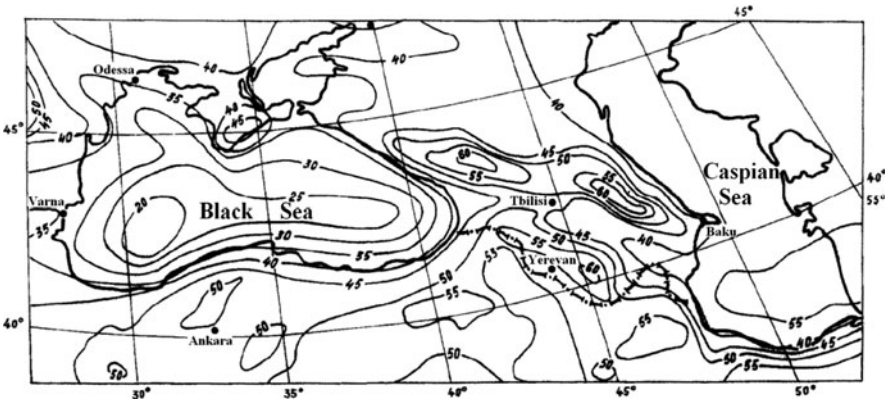


Fig. 2.21 Isodepths of the Moho discontinuity (in kilometers) in the Caucasus and adjacent regions (After Balavadze et al. 1979)

Based on the DSS data, this hidden basement arch explanation dominated. To test this hypothesis and reveal the Pre-Alpine basement, super-deep drilling was planned in the Saatly area, where the Kura and Araks Rivers merge. Examination of the gravity data (Tzimelzon 1970) and magnetic data analysis (Khesin et al. 1983) helped refine these predictions.

An upward continuation (recalculation onto the upper level) of the observed magnetic field to a height of 25 km contributed to showing that the Ganja regional

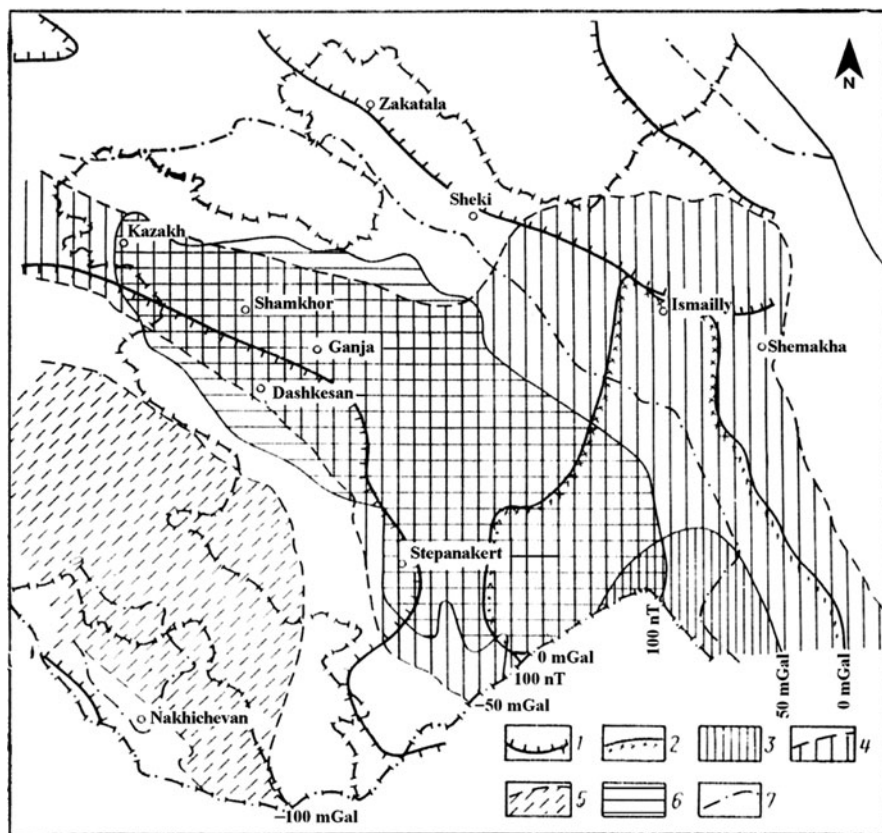


Fig. 2.22 Comparison of regional components of topography, gravity and magnetic fields (After Khesin 1976). (1) contour of regional mountain maxima of terrain relief; (2) zero isoline of the Bouguer regional maximum; (3) Bouguer intensive regional maximum (>50 mGal); (4) positive and moderately negative (down - 50 mGal) Bouguer regional field; (5) Bouguer intensive regional minimum (down - 100 mGal); (6) Ganja regional magnetic maximum; (7) zero isoline of the magnetic regional maximum

magnetic maximum primarily occupied the Middle Kura Depression and a significant part of the northeastern Lesser Caucasus (Khesin 1976). Regional components of the topography (elevation field) and gravity field were calculated as well (Fig. 2.22).

It is evident from Fig. 2.21 that the regional gravity maximum contains sub-meridian and sub-latitudinal components. A sub-meridian strike characterizes the most ancient crystalline complexes of the Talysh-Vandam (rather, the Talysh-Ismailly) maximum, whereas its western periphery is overlapped by the Ganja magnetic maximum of the Caucasian strike. Here, a common source of magnetic and gravity anomalies may be thick Mesozoic magmatic associations of increased magnetization and density at a depth of 3–4 km (Khesin 1976).

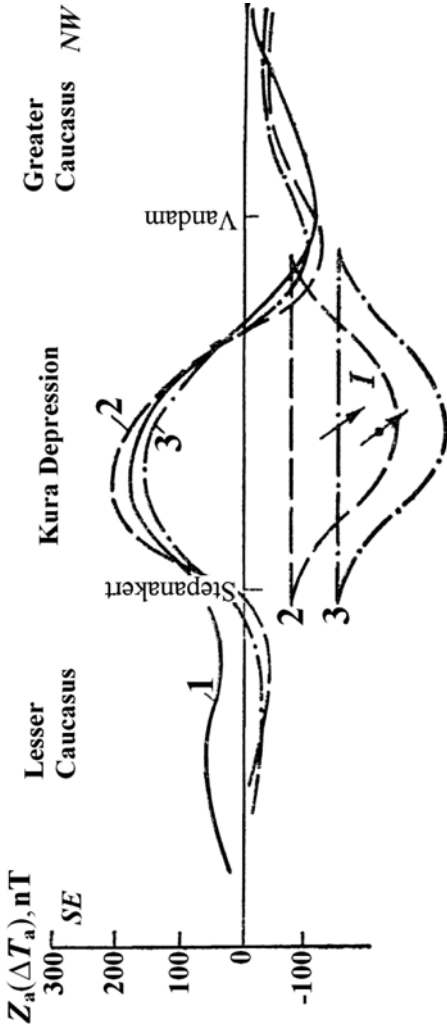


Fig. 2.23 Comparison of the results of upward continuation of the observed magnetic field to a height of 25 km (1) with modeled magnetic anomaly Z_a of the body occurring at a depth of 12.5 km (2) and 25 km (3) (After Khesin 1976, with modification). Arrows show location of the magnetization vector J

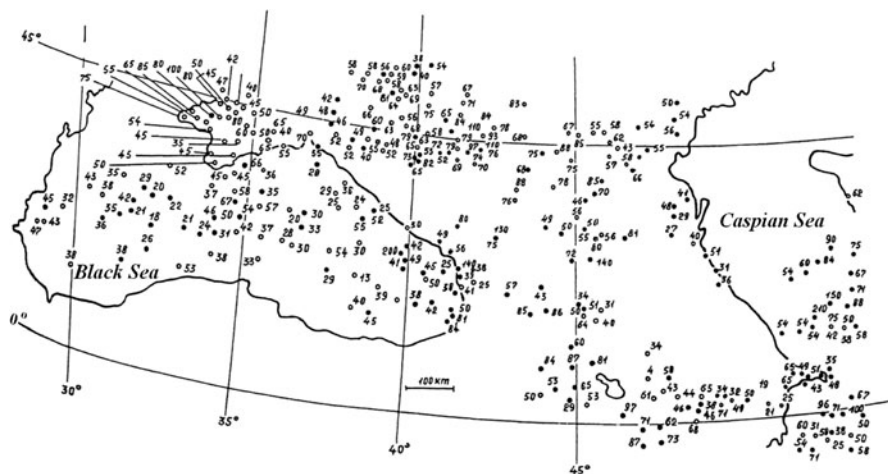


Fig. 2.24 Heat flow values at the Earth's surface for the Caucasus and adjoining areas (in mW/m^2) (After Alexidze et al. 1993, 1995)

A Ganja tectonic-magmatic zone with a Mesozoic magmatic section of basic-intermediate composition was predicted to unite the northeastern part of the Lesser Caucasus and the adjacent part of the Kura Depression which corresponds to the regional Ganja magnetic maximum (Khesin 1976). A simple magnetic model verified this supposition (Fig. 2.23).

Later, a buried arch of Mesozoic strata was confirmed by drilling at the depth predicted by the calculation of the location of the upper edge of the magnetic source. A super-deep (8.2 km) SD-1 borehole, drilled on the Saatly arch, revealed that under the Cenozoic and Upper Senonian sedimentary deposits there was a thick sequence of island-arc Cretaceous and Jurassic volcanic, ending at the bottom of the borehole with Upper Bajocian quartz plagioporphyres. This sequence is very similar to that of the adjacent part of the Lesser Caucasus. It thus confirmed the supposition of the Ganja tectonic-magmatic zone.

Nevertheless, sole reliance on seismic data led to mistakes in the planning of deep drilling as well. In the northern Caucasus, in the area of the Tyrnyauz molybdenum-wolfram deposit, a deep well was planned to reveal basement rocks under granites. However, Khesin's interpretation of the gravity minimum over this acid intrusive showed that its rocks of decreased density extended down to a depth of more than 5 km. In fact, the drilling was stopped in the granite less than 5 km to the well bottom.

At the same time, the application of several geophysical methods provided important information on the deep structure of the Caucasus. For example, on the basis of combining geothermic studies (e.g., Alexidze et al. 1993, 1995) (Fig. 2.24) with magnetotelluric sounding (MTS) and electro-telluric surveys certain deep electric and thermal specificities were revealed. According to Gugunava (1981, 1988), the Caucasian crust contains several electrically conducting units: (1) the

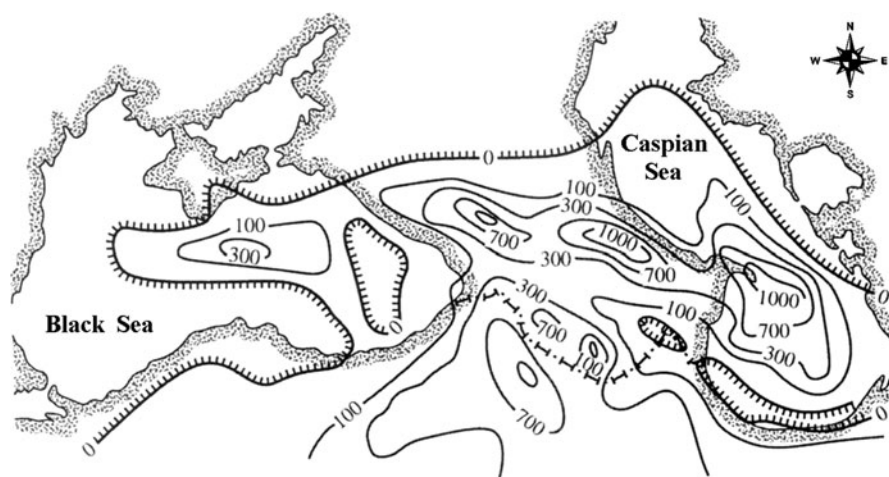


Fig. 2.25 Map showing the longitudinal conductance (in Siemens) of the crustal inverted layer in the Caucasus (After Gugunava 1988)

sedimentary cover (up to 15–20 km thick), (2) relicts of magma chambers within mountainous regions, and (3) the asthenosphere. This model was later confirmed by Spichak (1999). Chamber relicts were detected in the form of an oblate ellipsoid at a depth of about 20 km (Greater Caucasus) and as isolated lenses at a depth of 10–20 km (Lesser Caucasus). A crustal asthenosphere underlies the Transcaucasus (0–20 km thick) and attain maximal thickness beneath the Greater and Lesser Caucasus. High conductivity reflects the increased temperature at its depth; its highest values were detected in the southeastern prolongation of the Absheron Peninsula (Fig. 2.25), where increased geothermal gradients were measured (e.g., Khesin 1961; Kerimov et al. 1989).

More detailed deep structure according to the MTS data is shown for the chamber of the Elbrus volcano (Fig. 2.26).

Whereas the terrigenous cover within the adjacent Scythian Plate is characterized by low resistivity (for example, 1–2 and even 0.5–0.6 Ω m for the Maykopian deposits), volcanic rocks on the slopes of the Elbrus and its immediate vicinity show a resistivity $>1,000$ Ω m, and basement Proterozoic rocks and Paleozoic granites measuring hundreds to thousands of Ohm-meters. The upper crust resistivity in the Elbrus area decreases to 40–25 Ω m at a depth of 5–10 km. Another low-resistivity zone (25–15 Ω m in its center) in the middle and low crust propagates to a sub-crustal depth (exceeding 55 km). These conductivity anomalies have been linked to the magma and parent chambers and are most probably related to partial melting of rocks. This conclusion is consistent with the low velocities that were located using the reflected earthquake wave method at these depths, and with a density defect at a depth of 5–15 interpreted from the gravity minimum under Elbrus (Gurbanov et al. 2004).

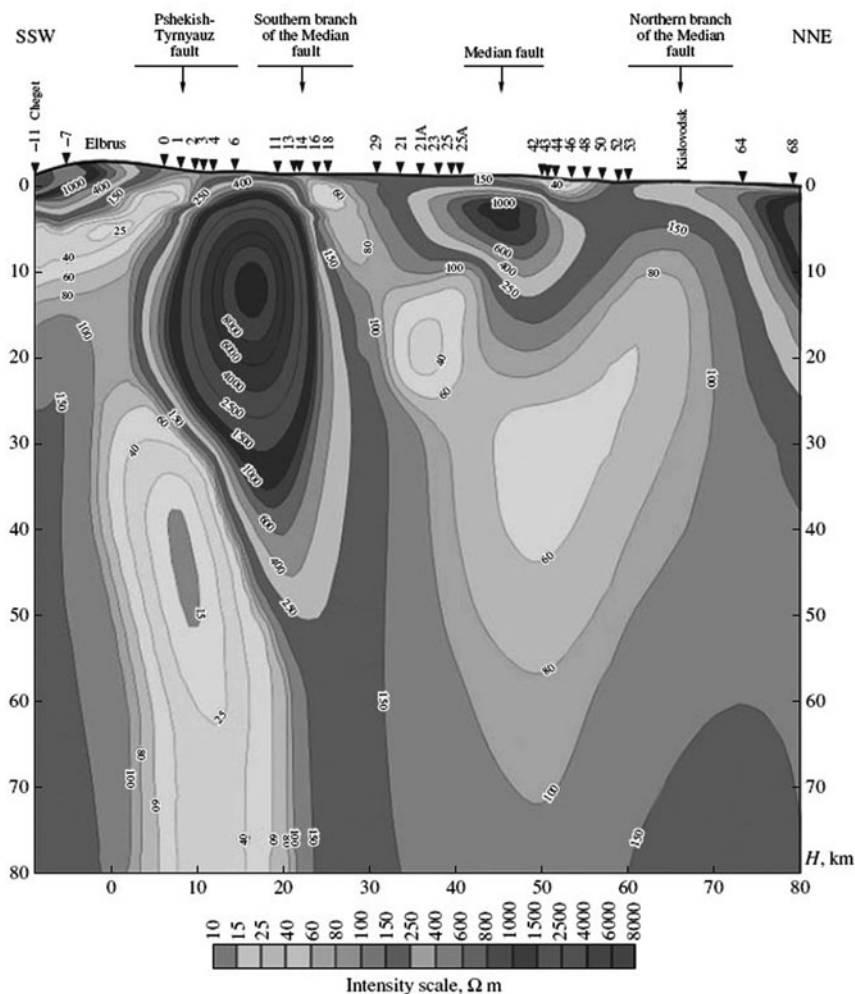


Fig. 2.26 The resistivity section according to MTS data along the North Elbrus profile (After Spichak et al. 2007)

At the same time, conductivity anomalies may be associated with deep faults. A high-gradient zone of conductivity in the interval of soundings No. 1 and No. 2 corresponds to the Pshekish-Tyrnyauz fault (Fig. 2.4), where highly mineralized fluids flow from the depths.

Paleomagnetic data are an important source for paleotectonic reconstructions (e.g., Gorodnitsky et al. 1978). The reduction of the location of the magnetic pole for different terranes at different times can serve to evaluate regional rotation and the relative displacement of these terranes. Issayeva and Khalafli (2006) carried out the last paleomagnetic study of this type. It was revealed that the regions of the

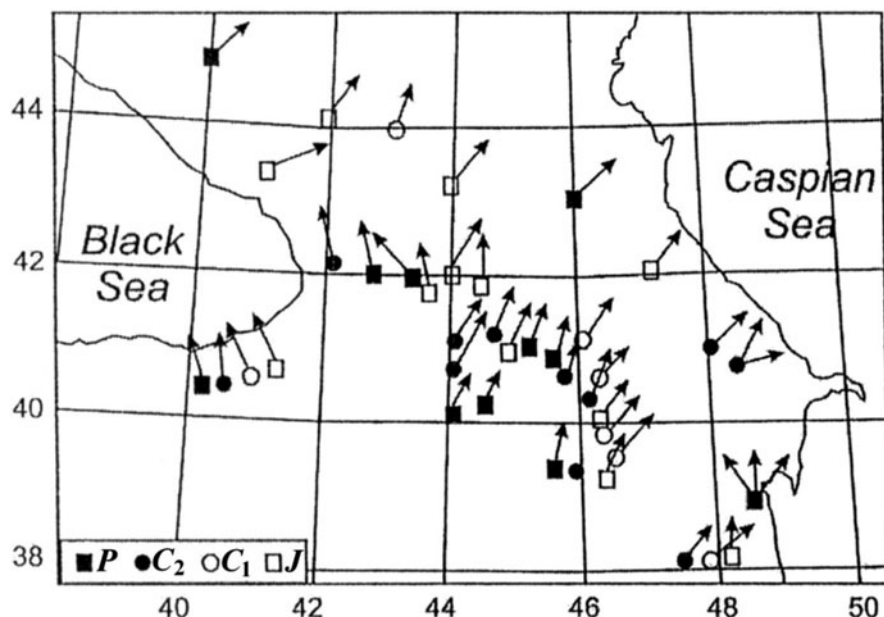


Fig. 2.27 Distribution of paleomagnetic vectors for the Mesozoic-Cenozoic rocks of the Lesser and Greater Caucasus, Iran and Turkey (After Issayeva and Khalafli 2006, with some modifications). *P* Paleogene, *C*₂ Late Cretaceous, *C*₁ Early Cretaceous, *J* Jurassic

Lesser and Greater Caucasus and Iran rotate clockwise through about 20–30° with respect to the magnetic meridian, and the North Anatolia rotates anticlockwise through about 30–40° (Fig. 2.27).

The average coordinates of the paleomagnetic poles for Azerbaijan, Georgia, Armenia, Turkey, and Iran were compared to the Russian platform and showed that these regions have been connected to the Eurasian continent since the Upper Eocene. The Lesser Caucasus has moved 5–7° to the south with respect to the Eurasian continent.



<http://www.springer.com/978-3-540-76618-6>

Geophysical Studies in the Caucasus

Eppelbaum, L.V.; Khesin, B.

2012, XVI, 404 p., Hardcover

ISBN: 978-3-540-76618-6